Journal of Radiation Research and Applied Sciences xxx (2014) 1–8

Available online at www.sciencedirect.com
ScienceDirect
Journal of Radiation Research and Applied Sciences
journal homepage: http://www.elsevier.com/locate/jrras

Influence of pH and glycine on the K X-ray fluorescence parameters of Zn and Cr in Zn–Cr alloys

M. Dogan [a,*], V. Aylikci [b], E. Tiraşoglu [a], İ.H. Karahan [c]

[a] Department of Physics, Faculty of Sciences, Karadeniz Technical University, 61080 Trabzon, Turkey
[b] Department of Metallurgy and Material Engineering, Faculty of Technology, Mustafa Kemal University, 31040 Hatay, Turkey
[c] Department of Physics, Faculty of Arts and Sciences, Mustafa Kemal University, 31040 Hatay, Turkey

ARTICLE INFO

Article history:
Received 6 March 2014
Received in revised form
24 March 2014
Accepted 25 March 2014
Available online xxx

Keywords:
Cross-sections
K X-ray intensity ratios
Charge transfer
Zn–Cr alloys
pH and glycine

ABSTRACT

In this study, $\sigma_{K\alpha,\beta}$ production cross-sections and K_β/K_α, intensity ratios of Cr and Zn have been measured in pure metals and in different alloy compositions which have different composition values. The alloying effects on the fluorescence parameters of Cr and Zn were investigated and the changes in these parameters interpreted according to the rearrangement of valance state electrons and the charge transfer process between the 3d elements which constitute the alloys. The samples were excited by 59.5 keV γ-rays from a ^{241}Am annular radioactive source. K X-rays emitted by samples were counted by an Ultra-LEGe detector with a resolution of 150 eV at 5.9 keV. The effect of pH and glycine values on alloy composition and alloying effect on the K x-ray fluorescence parameters of Cr and Zn were also investigated.

1. Introduction

The increasing application of alloys in various fields such as industry, agriculture, archaeology, etc. requires accurate knowledge of X-ray fluorescence parameters. In addition, comparison of measured K X-ray fluorescence cross-sections with theoretical estimates provides a check on validity of various physical parameters such as photoionization cross-section and fluorescence yields.

A great deal of investigation has been performed on experimental and theoretical K X-ray fluorescence parameters of 3d transition metals. Earlier theoretical values of fluorescence yield were obtained in the region $4 \leq Z \leq 54$ by McGuire (1969, 1970) and Walters and Bhalla (1971) using the Hartree–Fock–Slater model. Cu K x-ray production cross

* *Corresponding author*. Tel./fax: +90 462 3773502.
E-mail address: mdogan58@ktu.edu.tr (M. Dogan).
Peer review under responsibility of The Egyptian Society of Radiation Sciences and Applications

Production and hosting by Elsevier

http://dx.doi.org/10.1016/j.jrras.2014.03.004

Please cite this article in press as: Dogan, M., et al., Influence of pH and glycine on the K X-ray fluorescence parameters of Zn and Cr in Zn–Cr alloys, Journal of Radiation Research and Applied Sciences (2014), http://dx.doi.org/10.1016/j.jrras.2014.03.004

sections for 1.7-MeV/amu C, N, O, and F ions were determined in the limit of vanishingly thin solid Cu targets. The inclusion of electron transfer from the target K shell to the projectile in addition to direct ionization of the target in order to explain the charge-state and Z_1 dependences of the X-ray-production cross sections (Gardener et al., 1979). Kahoul, Abassi, Deghfel, and Nekkab (2011) calculated empirical K-shell fluorescence yields (ω_K) from the available experimental data for elements with $6 \leq Z \leq 99$. The experimental data are fitted using the quantity. There have been extensive experimental investigations on K_β/K_α X-ray intensity ratios and fluorescence yields of 3d transition elements (Be, Lepy, Plagnard, & Duchemin, 1998; Benall, Shidling, & Badiger, 2005; Brunner, Nagel, Hartmann, & Arndt, 1982; Casnati, Tartari, Baraldi, & Napoli, 1985; Çevik, Kaya, Ertugral, Baltas, & Karabıdak, 2007; Şimşek, Doğan, Turgut, & Ertuğral, 2000).

The binding energy of the valence electrons of an element, incorporated in different alloys has different values due to the change in the valence electrons participating in the formation of the chemical bond. As a result transition probabilities of a valance electron leading the variations in the K X-ray fluorescence parameters (Kalaycı et al., 2005). K_β/K_α X-ray intensity ratios of V and Ni in V_xNi_{1-x} alloys have been measured following excitation by 59.54 keV γ-rays from a 200 mCi ^{241}Am point-source. The experimental data indicate deviations of K_β/K_α intensity ratios for V and Ni in certain alloy compositions from the corresponding ratios for pure metals. These deviations indicate that the relative changes of the number of 3d electrons for V and Ni seem to be very similar if considered as functions of their own concentrations (Raj, Padhi, & Polasik, 1999). In Zn_xCo_{1-x} alloys (Aylıkcı et al., 2011), reduction the polarization depend on the changing the pH values of electrolyte. As a result of this dependence concentration of alloy composition is changed and this behavior causes an alloying effect on the K X-ray fluorescence parameters.

The change on the 3d electron population of both elements in different alloy composition is known to be alloying effect on the K X-ray fluorescence parameters. 3d electron population in the atom has a serious effect on the 3p orbitals more than the 2p orbitals which results in a change of the K_β/K_α X-ray intensity ratios. Because 3d and 4s levels are the valence state of 3d transition metals. These shells are far away from the nucleus respect to the inner shells (2p orbitals). Outer shells feel the attract force of nucleus more weakly than 2p orbitals and so alien element affect the valance shell more than inner shells. Therefore it can be said that K X-ray fluorescence parameters are a sensitive tool to investigate the electronic structure of 3d transition metals in alloys, compounds and complexes. Influence of the alloying effect on the K_β/K_α X-ray intensity ratios were investigated for Ti, Cr and Ni in Ti_xNi_{1-x} and Cr_xNi_{1-x} alloys (Bhuinya & Padhi, 1992), Fe and Ni in Fe_xNi_{1-x} alloys (Raj, Padhi, Polasik, Pawlowski, & Basa, 2000), Ti, Cr, Fe and Co in their alloys (Pawlowski et al., 2002). The changes between the experimental and theoretically values of elements constitutes the alloys can be explained by assuming rearrangement of electrons between 3d and (4s, 4p) valence band states of the individual metal atoms. In addition to these studies, the alloying effect on the K shell fluorescence yield was investigated for Cr, Ni and Al elements in Cr_xNi_{1-x} and Cr_xAl_{1-x} alloys (Büyükkasap, 1998). Raj, Padhi, Polasik, Pawlowski, and Basa (2001) irradiated the Fe_xNi_{1-x} alloys due to the rapid advance of magnetoelectronics. Valance electronic structure of Fe and Ni in Fe–Ni alloys calculated using the results obtained from K_β/K_α X-ray intensity ratios. K and L shell X-ray fluorescence parameters of Co, Cu and Ag in pure metals and different alloy compositions were determined using EDXRF by Aylıkcı et al. (2009). $\sigma_{L\beta}$, $\sigma_{L\alpha}$ of Ag and $\sigma_{K\beta}$, $\sigma_{K\alpha}$ of Co and Cu X-ray production cross sections values compared with theoretical values. It was explained the alloying effect using the changes on the X-ray florescence parameters. For the Cr, Zr, Nb, V, W, Mo and Al elements, the alloying effect on the trend of elastic properties of TiN-based nitrides have been investigated using ab initio density functional theory calculations within the generalized gradient approximation (Chen, Zhao, Rodgers, & Tse, 2003). The valence-electron structure of Ti and Co in the Ti_xCo_{1-x} were calculated by the comparison of the measured $K\alpha$-to-$K\beta$ x-ray intensity ratios with the results of multiconfiguration Dirac–Fock calculations for various electron structures of these metals (Han & Demir, 2010).

In this paper, Zn and Cr elements in the different alloy composition were measured by the EDXRF system. The $\sigma_{K\beta}$ production cross-sections and K_β/K_α X-ray intensity ratios of these elements in Zn_xCr_{1-x} alloys was investigated and the obtained values were interpreted according to the rearrangement process of the valance state.

2. Experimental procedure

2.1. Electrodeposition of Zn–Cr alloys

$Zn_{1-x}Cr_x$ alloys have been electrodeposited with an approximate thickness of 2 μm on aluminum foils from chloride baths at room temperature. The working electrodes were aluminum foils and AISI 4140 steel disks. All these electrolytes were prepared from Merck pro-analysis grade chemicals using double-distilled water and consisted of $ZnCl_2$ 67.5 gl^{-1}, N_2HCH_2COOH 200 gl^{-1}, H_3BO_3 31.5 gl^{-1}, NH_4Cl 95.4 gl^{-1}, $CrCl_3 \cdot 6H_2O$ 160 gl^{-1} for the Zn–Cr alloys (Table 1).

The measured quantity for the pH and glycine was adjusted according to Table 1. The plating time was 15 min, after which the cathode was withdrawn, washed with distilled water and dried. The deposition potential was −1.5 V.

Before electrodeposition, aluminum foils were mechanically polished with silicon carbide emery paper, degreased in 1 M NaOH with surfactant at 70 °C during 5 min and finally rinsed with the twice distilled water (18 MΩ cm) and dried in air. Counter electrode was a Pt electrode, for the polarization and the corrosion measurements. The reference electrode used in all experiments was a saturated calomel electrode (SCE). All the potentials are referred against SCE. The electrodeposition of alloys was performed with an electrochemical analyzer/workstation (Model 1100, CH Instruments USA) with a three-electrode configuration realized at room temperature in a Pyrex glass cell. The exposed area of the specimens was about 1 cm^2 (Doğan et al., 2013). The agreement of lattice parameters with reported values confirms that films are hexagonal and polycrystalline.

Please cite this article in press as: Dogan, M., et al., Influence of pH and glycine on the K X-ray fluorescence parameters of Zn and Cr in Zn–Cr alloys, Journal of Radiation Research and Applied Sciences (2014), http://dx.doi.org/10.1016/j.jrras.2014.03.004

Table 1 – Solutions compositions for the alloy electrodeposition.

Solutions compositions	Zn_xCr_{1-x} (x = 98.5, 98.9, 98.2, 99.3)	Zn_xCr_{1-x} (x = 97.5, 97, 98)
$ZnCl_2$ (gl^{-1})	67.5	67.5
$CrCl_36H_2O$ (gl^{-1})	160	160
N_2HCH_2COOH (gl^{-1})	200	200
H_3BO_3 (gl^{-1})	31.5	31.5
NH_4Cl (gl^{-1})	95.4	95.4
Glycine (g)	–	0.004, 0.008, 0.012
Solution pH	2, 2.5, 3, 3.5	3
Deposition time (min)	15	15
Voltage (V)	−1.5	−1.5

2.2. X ray fluorescence analysis

The geometry of the experimental set-up and the present experimental equipments has been described in Fig. 1. In order to reduce the statistical error in the experimental measurements, the measurements were repeated three times on the same target and the spectra were analyzed by using Origin software program. In the experimental determinations, spectral deconvolution is one of the main problems that arise when determining these parameters due to the strong peak overlapping in ED-XRF system. Good statistics is necessary for this purpose and a careful fitting methodology is required in order to obtain accurate values for the peak areas. In this experimental set-up, 59.5 keV gamma photons emitted by an annular 50 mCi ^{241}Am radioactive source were used. The fluorescence K X-rays from the sample were detected by a collimated Ultra-LEGe detector having a thickness of 5 mm and an energy resolution of 150 eV at 5.96 keV. Fig. 2 Zn K X-ray spectrum for the $Zn_{0.97}Cr_{0.03}$ alloy. The r^2 value can be inspected and this value is almost 0.99 for the whole range and measurements. The residue spectrum concerns the peak determining process. If it is desired to know the main peak, the hidden peak or peaks, the residue spectra have to be checked out carefully.

The K_i X-ray production cross-sections were obtained by using the following relation:

$$\sigma_{K_i} = \frac{N_{K_i}}{I_0 G \varepsilon_{K_i} \beta_{K_i} m} \quad (i = \alpha \text{ and } \beta) \tag{1}$$

where N_{K_i} is the measured intensity (area under the photo-peak) corresponding to the K_i X-rays, I_0 is the intensity of the incident radiation, G is the geometric factor, ε_{K_i} is the detection efficiency for the K_i X-rays and β_{K_i} is the self-absorption correction factor for the target material, which accounts for the absorption in the target of the incident photons and the emitted characteristic X-rays. m is the thickness of the target in g/cm^2.

The self absorption correction was calculated using the equation:

$$\beta = \frac{1 - \exp\{[-(\mu_{inc} \cos\theta_1 + \mu_{emt} \cos\theta_2)m]\}}{(\mu_{inc} \cos\theta_1 + \mu_{emt} \cos\theta_2)m} \tag{2}$$

where μ_{inc} is the mass attenuation coefficient (cm^2/g) of incident photons and μ_{emt} is of emitted characteristic X-rays (Berger & Hubbell, 1999). The angles of incident photons and emitted X-rays with respect to the surface of the samples, θ_1 and θ_2, were equal to 45° and 90° in the present experimental set-up, respectively. m is the thickness of the target in g/cm^2.

The product $I_0G\varepsilon$, containing the terms related to the incident photon flux, geometrical factor and absolute efficiency of the X-ray detector, was determined by collecting the K_α and K_β X-ray spectra of samples of Cr, Fe, Zn, As, Se, Sr, Zr, Mo, Ru and Cd in the same geometry using the equation:

$$I_0 G \varepsilon_{K_i} = \frac{N_{K_i}}{\sigma_{K_i} \beta_{K_i} m} \quad (i = \alpha \text{ and } \beta) \tag{3}$$

The terms are the same meaning as Eq. (1). The factor $I_0G\varepsilon_{K_i}$ was fitted as a function of energy using the equations.

The factor $I_0G\varepsilon_{K_i}$ was fitted as a function of energy using the equations

$$I_0 G \varepsilon_{K_i} = A_0 + A_1 E_x + A_2 {E_x}^2 + A_3 {E_x}^3 \quad \text{(1st part)} \tag{4}$$

$$I_0 G \varepsilon_{K_i} = B_0 + B_1 E_x + B_2 {E_x}^2 \quad \text{(2nd part)} \tag{5}$$

where E_x is the K_α and K_β X-ray energy and A_0, A_1, A_2, A_3, B_0, B_1 and B_2 are constants evaluated from a fitting polynomial. The variation of the factor $I_0G\varepsilon_{K_i}$ as a function of the mean K X-ray energy is shown in Fig. 3. The Eqs. (4) and (5) correspond to the left hand side and right hand side of the Fig. 3 respectively.

Theoretical values of the σ_{K_i} X-ray production cross-sections were calculated using the following equation:

$$\sigma_{K_i} = \sigma_K(E) \omega_K F_{K_i} \tag{6}$$

where $\sigma_K(E)$ is the K-shell photoionization cross-section of the given element for the excitation energy E (Scofield, 1973), ω_K is the K-shell fluorescence yield (Krause, 1979), and F_{K_i} is the emission rate of the fractional X-ray for K_α and K_β X-rays (Broll, 1986).

3. Result and discussion

The $\sigma_{K\alpha}$ and $\sigma_{K\beta}$ production cross-sections and K_β/K_α X-ray intensity ratios of Zn and Cr for different Zn_xCr_{1-x} alloy composition (x = 0.985, 0.989, 0.982, 0.993, 0.975, 0.970, 0.980) changing with the pH and glycine values have been tabulated in Tables 2 and 3.

The experimental values presented in Table 2 point out that the $\sigma_{K\alpha}$ X-ray production cross-section values do not change much relative to experimental error limits and are not affected by the physical and chemical environment of the investigated elements. This could be because that the K_α X-ray emissions consist of the ($L_{2,3} \rightarrow K$) transitions and these sub-shells are far from the valance bands of Cr and Zn elements. The valance states of these elements are composed of the M_4, M_5 and N_1 sub-shells (Cengiz et al., 2010).

The increment of pH and glycine values changes the composition of alloys. Elemental composition of the solution is affected the dissolving molecules in the composite. Generally, it can be seen from the Table 1 for the alloys changing with the pH values, deposition of the zinc atoms is

Please cite this article in press as: Dogan, M., et al., Influence of pH and glycine on the K X-ray fluorescence parameters of Zn and Cr in Zn–Cr alloys, Journal of Radiation Research and Applied Sciences (2014), http://dx.doi.org/10.1016/j.jrras.2014.03.004

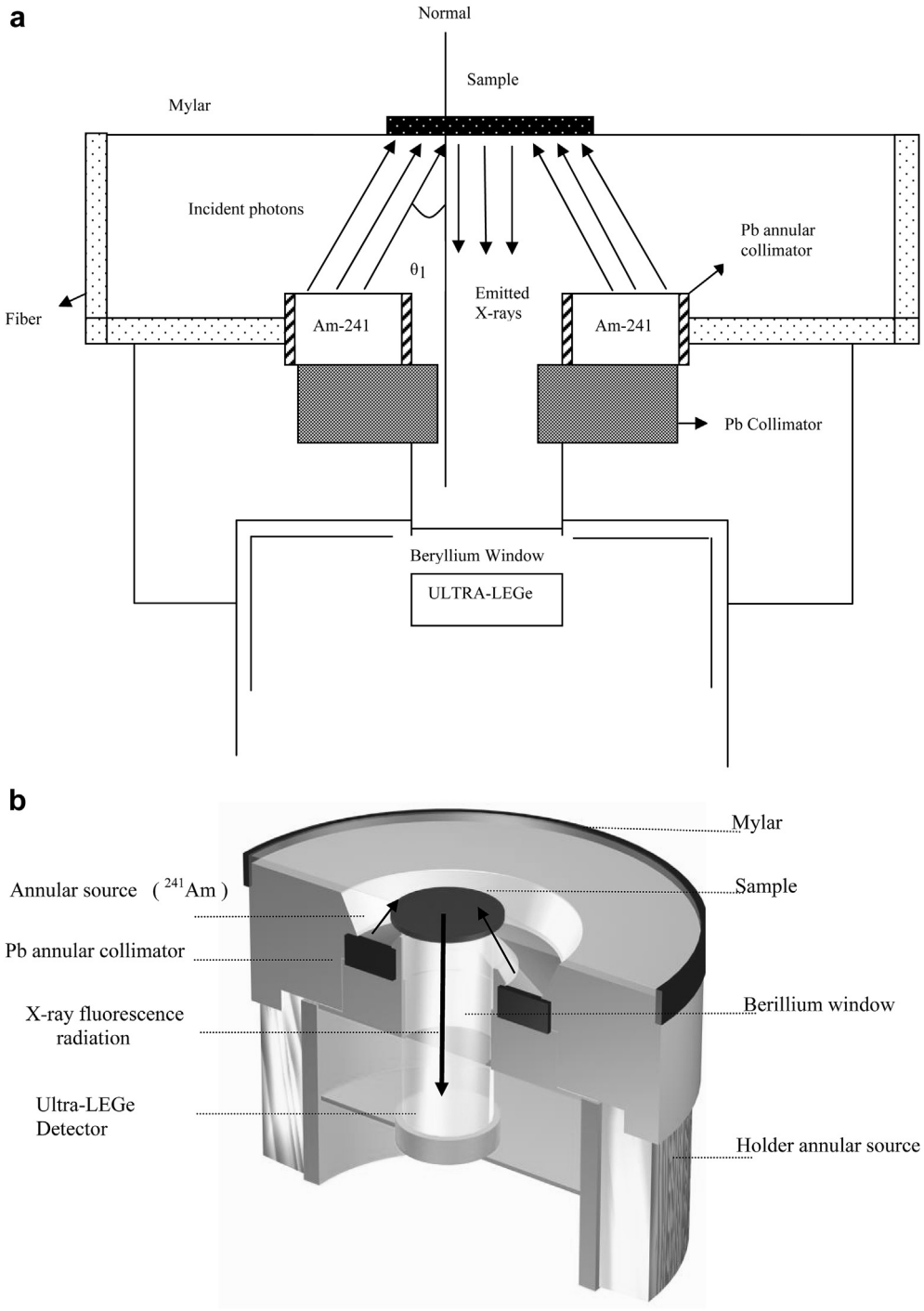

Fig. 1 – a) Geometry of experimental set up. b) A closer look for annular source.

proportional to pH values of solution. The hydrogen evolution affects directly the acidity of the solution and this causes the changes on the redox potential and cathode current efficiency. For the alloys changing with glycine values, increasing of the glycine causes the decrement of zinc concentration or increment of chromium concentration. Because increment of glycine absorbs the hydrogen and zinc atoms in the solution and so mobility of the solution decreases. This decrement affects the cathode polarization which is responsible the deposition of zinc and chromium atoms.

As seen from Table 2, the $\sigma_{K\beta}$ production cross-sections values of Zn and Cr elements in the Zn_xCr_{1-x} alloys are different from theoretical values (Scofield, 1974) for pure elements. For the samples with 2, 2.5, 3 and 3.5 pH values, we find about 20.8%, 17.8%, 23.3% and 11.1% increase in the $\sigma_{K\beta}$ cross-section values of Zn, respectively. For the samples with 0.004,

Please cite this article in press as: Dogan, M., et al., Influence of pH and glycine on the K X-ray fluorescence parameters of Zn and Cr in Zn–Cr alloys, Journal of Radiation Research and Applied Sciences (2014), http://dx.doi.org/10.1016/j.jrras.2014.03.004

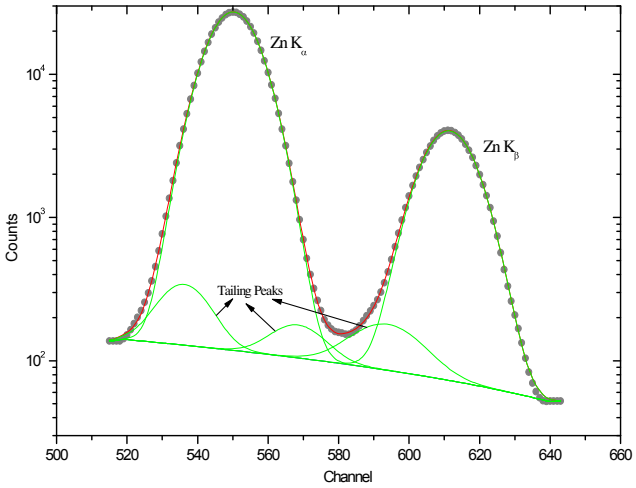

Fig. 2 – Typical Zn K X-ray spectrum for alloy $Zn_{0.97}Cr_{0.03}$.

0.008 and 0.012 glycine values, we find about 27.3%, 28.5% and 25.6% increase in the $\sigma_{K\beta}$ cross-section values of Zn, respectively. In addition to, for the samples with 2, 2.5, 3 and 3.5 pH values, we find about 31.7%, 28.9%, 35.3% and 20.2% decrease in the $\sigma_{K\beta}$ cross-section values of Cr, respectively. For the samples with 0.004, 0.008 and 0.012 glycine values, we find about 41.9%, 43.9% and 38.4% decrease in the $\sigma_{K\beta}$ cross-section values of Cr, respectively.

Similar results can be observed for K_β/K_α X-ray intensity ratio values on the Table 3. For Cr, the measured experimental values are lower than the calculated theoretical values and these changes are between the 21.3% and 41.6%. On the contrary, for Zn element, K_β/K_α X-ray intensity ratio values are higher than theoretical values and these changes are between the 6% and 34%.

It is very well known that metallic bonding such as alloys and metallic components usually consist of the two or more transition metals. Characterization of the bonding is determined by the how to be affected the valance electron

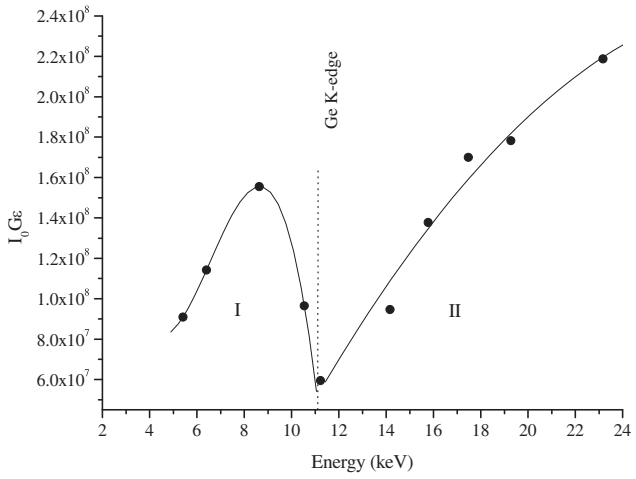

Fig. 3 – The variation of the factor $I_0G\varepsilon$ as a function of the mean K X-ray energy.

Table 2 – The experimental $\sigma_{K\alpha}$, $\sigma_{K\beta}$ production cross-sections of Cr and Zn in the pure metals and in the different alloy compositions.

Sample	Constitution element	pH	Glycine	Present work	$\sigma_{K\alpha}$ (cm^2/g)			Present work	$\sigma_{K\beta}$ (cm^2/g)		
					Theoretical	Calculated			Theoretical	Calculated	
						Semi-empirical[a]	Semi-empirical[b]			Semi-empirical[a]	Semi-empirical[b]
Zn	Zn	–	–	0.587 ± 0.030	0.600[a]	0.585[b]	0.582[b]	0.0717 ± 0.0036	0.0742[a]	0.0724[b]	0.0719[b]
Cr	Cr	–	–	0.170 ± 0.009	0.179[a]	0.170[b]	0.171[b]	0.0201 ± 0.0010	0.0210[a]	0.0200[b]	0.0201[b]
$Zn_{0.985}Cr_{0.015}$	Zn	2	–	0.62425 ± 0.03184				0.08961 ± 0.00457			
	Cr			0.17129 ± 0.00874				0.01432 ± 0.00073			
$Zn_{0.989}Cr_{0.011}$	Zn	2.5	–	0.62503 ± 0.03188				0.08743 ± 0.00446			
	Cr			0.17252 ± 0.00880				0.01355 ± 0.00069			
$Zn_{0.982}Cr_{0.018}$	Zn	3	–	0.62919 ± 0.03209				0.0915 ± 0.00467			
	Cr			0.18651 ± 0.00951				0.01491 ± 0.00076			
$Zn_{0.993}Cr_{0.007}$	Zn	3.5	–	0.62639 ± 0.03195				0.08246 ± 0.00421			
	Cr			0.18449 ± 0.00941				0.01673 ± 0.00085			
$Zn_{0.975}Cr_{0.025}$	Zn	3	0.004	0.57864 ± 0.02951				0.09444 ± 0.00481			
	Cr			0.17099 ± 0.00872				0.01218 ± 0.00062			
$Zn_{0.97}Cr_{0.03}$	Zn	3	0.008	0.57182 ± 0.02916				0.09534 ± 0.00486			
	Cr			0.17460 ± 0.00891				0.01177 ± 0.00600			
$Zn_{0.98}Cr_{0.02}$	Zn	3	0.012	0.57086 ± 0.02911				0.09318 ± 0.00475			
	Cr			0.18711 ± 0.00954				0.01290 ± 0.00066			

[a] Scofield (1974).
[b] Aylıkcı et al. (2011).

Please cite this article in press as: Dogan, M., et al., Influence of pH and glycine on the K X-ray fluorescence parameters of Zn and Cr in Zn–Cr alloys, Journal of Radiation Research and Applied Sciences (2014), http://dx.doi.org/10.1016/j.jrras.2014.03.004

Table 3 – The experimental K_β/K_α intensity ratios of Cr and Zn in the pure metals and in the different alloy compositions.

Sample	Constitution element	pH	Glycine	K_β/K_α intensity ratios						
				Present work	Calculated		Theoretical	Electronic Configuration	Theoretical (Polasik, 1998)	
					Empirical	Semiempirical			Coulomb Gauge	Babushkin Gauge
Zn	Zn	–	–	0.1221 ± 0.0062	0.1338[b]	0.1365[b]	0.1241[a]	–	–	–
Cr	Cr	–	–	0.1182 ± 0.0060	0.1324[b]	0.1276[b]	0.1153[a]	$3d^44s^2$	0.1333[c]	0.1354[c]
								$3d^54s^1$	0.1295[c]	0.1317[c]
								$3d^6$	0.1268[c]	0.1289[c]
$Zn_{0.985}Cr_{0.015}$	Zn	2	–	0.14355 ± 0.00732						
	Cr			0.08362 ± 0.00426						
$Zn_{0.989}Cr_{0.011}$	Zn	2.5	–	0.13988 ± 0.00713						
	Cr			0.08643 ± 0.00441						
$Zn_{0.982}Cr_{0.018}$	Zn	3	–	0.14543 ± 0.00741						
	Cr			0.07266 ± 0.00370						
$Zn_{0.993}Cr_{0.007}$	Zn	3.5	–	0.13164 ± 0.00671						
	Cr			0.09071 ± 0.00462						
$Zn_{0.975}Cr_{0.025}$	Zn	3	0.004	0.16321 ± 0.00832						
	Cr			0.07123 ± 0.00363						
$Zn_{0.97}Cr_{0.03}$	Zn	3	0.008	0.16673 ± 0.00849						
	Cr			0.06739 ± 0.00343						
$Zn_{0.98}Cr_{0.02}$	Zn	3	0.012	0.16322 ± 0.00832						
	Cr			0.06895 ± 0.00351						

[a] Scofield (1974).
[b] Aylıkcı et al. (2011).
[c] Polasik (1998).

Please cite this article in press as: Dogan, M., et al., Influence of pH and glycine on the K X-ray fluorescence parameters of Zn and Cr in Zn–Cr alloys, Journal of Radiation Research and Applied Sciences (2014), http://dx.doi.org/10.1016/j.jrras.2014.03.004

structure from the neighboring element. Especially, outer shell electrons or valance electrons are free to move throughout the metal or alloy in a metallic bond. Valance shell will be more affected than the core shells because of shortening the distance between the two or more atoms in the alloys and this situation causes a serious effect on the $\sigma_{K\beta}$ production cross-sections and K_β/K_α X-ray intensity ratios. This can be explained the two mechanism. Firstly, the charge transfer mechanism from one element to other can be explained by the electronegativity values of Cr and Zn. During the charge transfer from Zn to Cr, screening effect on the outer shell electrons will increase and the binding energy of the outer shell of Cr will decrease. The decreasing of the bonding energies of the outer shell electrons causes a decreasing on the K X-ray transition probability but the opposite effect is observed for Zn which the electrons are removed from it. The second and predominant mechanism is the rearrangement of valance electrons because of the unfilled states of chromium element. The valance electron structure was affected by the changing of 3d electron population and this is responsible to the decrement the K_β/K_α X-ray intensity ratios with the increment of 3d electron number for Cr element in the different alloy compositions. In Table 3, it can be seen that the different electron configuration for chromium.

The uncertainties in the measurements are estimated to be less than 6% and are found propagating the errors in various parameters used for determination of X-ray parameters. The uncertainties in these parameters of counting statistic $N(K_i)$ ($i = \alpha, \beta$) errors in different parameters used to evaluate factor $I_0 G \varepsilon_{K_i}$, error in the absorption coefficients at incident and emitted photon energies, non-uniform thickness m are 3%, 2%, 3%, 2%, respectively.

4. Conclusion

In this study, it is shown that pH and glycine values change the concentration of alloy compositions and this behavior causes an alloying effect. We have found that the alloying effect is generally significant in the case of the investigated alloys and is reflected in the changes of the $\sigma_{K\beta}$ production cross-sections and K_β/K_α X-ray intensity ratios. By comparing the measured K X-ray fluorescence parameters with the Scofield's (1974) theoretical values showed that valance shell electrons were more affected than the inner shell electrons. This effect was tried to explain the charge transfer mechanism and rearrangement process of the outer shell electrons in the 3d and 4s shells.

REFERENCES

Aylıkcı, N. K., Aylıkcı, V., Kahoul, A., Tirasoglu, E., Karahan, İ.,H., & Cengiz, E. (2011). Effect of pH treatment on K-shell intensity ratios and K-shell x-ray production cross sections in ZnCo alloys. *Physical Review A, 84*, 1–10.

Aylıkcı, N. K., Tıraşoğlu, E., Apaydın, G., Cengiz, E., Aylıkcı, V., & Bakkaloğlu, Ö. F. (2009). Influence of alloying effect on x-ray florescence parameters of Co and Cu in CoCuAg alloy films. *Chemical Physics Letters, 475*, 135–140.

Be, M. M., Lepy, M. C., Plagnard, J., & Duchemin, B. (1998). Measurement of relative X-ray intensity ratios for elements in the $22 \leq Z \leq 29$ region. *Applied Radiation and Isotopes, 49*, 1367–1372.

Benall, A. S., Shidling, P. D., & Badiger, N. M. (2005). Measurements of K x-ray fluorescence parameters. *American Journal of Physics, 73*, 883–892.

Berger, M. J., & Hubbell, H. J. (1999). XCOM: Photon cross-sections on a personnel computer (version 1.2) NBSIR85-3597 National Bureau of Standards, Gaithersburg MD USA for version 3.1 see http://physics.nist.gov/.

Bhuinya, C. R., & Padhi, H. C. (1992). Alloying effect on the K_β/K_α intensity ratios of Ti, Cr and Ni. *Journal of Physics B: Atomic and Molecular Physics, 25*, 5283–5287.

Broll, N. (1986). Quantitative X-ray fluorescence analysis theory and practice of the fundamental coefficient method. *X-Ray Spectrometry, 15*, 271–285.

Brunner, G., Nagel, M., Hartmann, E., & Arndt, E. (1982). Chemical sensitivity of the K_β/K_α, X-ray intensity ratio for 3d elements. *Journal of Physics B: Atomic and Molecular Physics, 15*, 4517–4522.

Büyükkasap, E. (1998). Analytical note alloying effect on K shell fluorescence yield in Cr_xNi_{1-x} and Cr_xAl_{1-x} alloys. *Spectrochimica Acta Part B, 53*, 499–503.

Casnati, E., Tartari, A., Baraldi, C., & Napoli, G. (1985). Measurement of the K_β/K_α yield ratios of Cu, Mo and Cd stimulated by 59.54 keV photons. *Journal of Physics B: Atomic and Molecular Physics, 18*, 2843–2849.

Cengiz, E., Bıyıklıoğlu, Z., Aylıkcı, N. K., Aylıkcı, V., Apaydın, G., Tıraşoğlu, E., et al. (2010). Chemical effect on K shell x-ray fluorescence parameters and radiative Auger ratios of Co, Ni, Cu, and Zn complexes. *Chinese Journal of Chemical Physics, 23*, 138–144.

Çevik, U., Kaya, S., Ertugral, B., Baltas, H., & Karabıdak, M. (2007). K-shell X-ray fluorescence cross-sections and intensity ratios for some pure metals at 59.5 and 123.6 keV. *Nuclear Instruments and Methods in Physics Research Section B, 262*, 165–170.

Chen, K., Zhao, L. R., Rodgers, J., & Tse, J. S. (2003). Alloying effects on elastic properties of TiN-based nitrides. *Journal of Physics D: Applied Physics, 36*, 2725–2729.

Doğan, M., Tıraşoğlu, E., Karahan, İ. H., Aylıkçı, N. K., Aylıkçı, V., Kahoul, A., et al. (2013). Alloying effect on K X-ray intensity ratios and production cross section values of Zn and Cr in Zn–Cr alloys. *Radiation Physics and Chemistry, 87*, 6–15.

Gardner, R. K., Gray, T. J., Richard, P., Schmiedekamp, C., Jamison, K. A., & Hall, J. M. (1979). Cu K x-ray production as a function of projectile atomic number, energy, and incident charge state. *Physical Review A, 19*, 1896–1899.

Han, İ., & Demir, L. (2010). Relative K X-ray intensity studies on valance-electron structure of Ti and Co in Ti_xCo_{1-x} alloys. *Physical Review A, 82*, 1–5, 042514.

Kahoul, A., Abassi, A., Deghfel, B., & Nekkab, M. (2011). K-shell fluorescence yields for elements with $6 \leq Z \leq 99$. *Radiation Physics and Chemistry, 80*, 369–377.

Kalayci, Y., Agus, Y., Ozgur, S., Efe, N., Zararsiz, A., Arikan, P., et al. (2005). Influence of alloying effect on nickel fluorescence yield in Ni–Si alloys. *Spectrochimica Acta Part B, 60*, 277–279.

Krause, M. O. (1979). Atomic radiative and radiationless yields for K and L shells. *Journal of Physical and Chemical Reference Data, 8*, 307–327.

McGuire, E. J. (1969). K-shell Auger transition rates and fluorescence yields for elements Be–Ar. *Physical Review, 185*, 1–6.

McGuire, E. J. (1970). K-shell Auger transition rates and fluorescence yields for elements Ar–Xe. *Physical Review A, 2*, 273–278.

Pawłowski, F., Polasik, M., Raj, S., Padhi, H. C., & Basa, D. K. (2002). Valence electronic structure of Ti, Cr, Fe and Co in some alloys

Please cite this article in press as: Dogan, M., et al., Influence of pH and glycine on the K X-ray fluorescence parameters of Zn and Cr in Zn–Cr alloys, Journal of Radiation Research and Applied Sciences (2014), http://dx.doi.org/10.1016/j.jrras.2014.03.004

from K_β/K_α X-ray intensity ratio studies. *Nuclear Instruments and Methods in Physics Research Section B, 195*, 367–373.

Polasik, M. (1998). Influence of changes in the valence electronic configuration on the K_b-to-K_a X-ray intensity ratios 3d transition metals. *Physical Review A, 58*, 1840–1845.

Raj, S., Padhi, H. C., & Polasik, M. (1999). Influence of alloying effect on K_β/K_α X-ray intensity ratios of V and Ni in V_xNi_{1-x} alloys. *Nuclear Instruments and Methods in Physics Research Section B, 155*, 143–152.

Raj, S., Padhi, H. C., Polasik, M., Pawlowski, F., & Basa, D. K. (2000). Valence electronic structure of Fe and Ni in Fe_xNi_{1-x} alloys from relative K x-ray intensity studies. *Solid State Communications, 116*, 563–567.

Raj, S., Padhi, H. C., Polasik, M., Pawlowski, F., & Basa, D. K. (2001). Kβ-to-Kα x-ray intensity ratio studies of the valance electronic structure of Fe and Ni in Fe_xNi_{1-x} alloys. *Physical Review B, 63*, 1–4, 073109.

Scofield, J. H. (1973). *Theoretical photoionization cross section from 1 keV to 1500 keV* (Vol. 51326). Lawrence Livermore Laboratory (UCRL).

Scofield, J. H. (1974). Exchange corrections of K X-ray emission rates. *Physical Review A: Atomic, Molecular and Optical Physics, 9*, 1041–1047.

Şimşek, Ö., Doğan, O., Turgut, Ü., & Ertuğral, M. (2000). Measurement of K shell fluorescence yields of some elements in the atomic range $22 \leq Z \leq 30$ using photoionization. *Radiation Physics and Chemistry, 58*, 207–211.

Walters, D. L., & Bhalla, C. P. (1971). Nonrelativistic Auger rates, X-ray rates, and fluorescence yields for the 2p shell. *Physical Review A, 3*, 2164–2170.

Please cite this article in press as: Dogan, M., et al., Influence of pH and glycine on the K X-ray fluorescence parameters of Zn and Cr in Zn–Cr alloys, Journal of Radiation Research and Applied Sciences (2014), http://dx.doi.org/10.1016/j.jrras.2014.03.004